Journal of Petroleum Science and Technology 10 (2020) 20-30
DOI:10.22078/jpst.2020.4065.1651

Journal of Petroleum Science and Technology

https://jpst.ripi.ir/

A New Model for Permeability Estimation In Carbonate Reservoirs By Using NMR T_2 Distribution and Lsboost Ensemble Technique

Shahin Parchekhari [1,2], Ali Nakhaee [1,3*] and Ali Kadkhodaie[4]

1 Department of Petroleum Engineering, Kish International Campus, University of Tehran, Kish, Iran

2 Petroleum Engineering Department, National Iranian Southfield Oil Company (NISOC), Ahvaz, Iran

3 Institute of Petroleum Engineering, School of Chemical Engineering, College of Engineering, University of Tehran, Tehran, Iran

4 Earth Sciences Department, University of Tabriz, Tabriz, Iran

Abstract

Permeability is arguably the most critical property for evaluating flow in the reservoir. It is also one of the challenging parameters which must be measured in the field. Nuclear Magnetic Resonance (NMR) logging across the borehole is among the popular techniques, which it is utilized to determine permeability across the reservoir. However, available correlations in literature for estimating permeability from NMR data do not usually provide acceptable accuracy in the carbonate rocks. Therefore, a new model is proposed to estimate permeability by establishing a relationship between core derived permeability and extracted features from the T_2 distribution curve of NMR data with the ensemble LSBoost algorithm. The feature extraction process is performed using peak analysis on T_2 distribution curves which it leads to 5 relevant parameters, including T_{2lm}, TCMR, prominence, peak amplitude and width. The proposed model is validated by comparing the proposed method's correlation coefficient against Timur-Coates and SDR equation estimation accuracy. The results show that our model generally provides better prediction accuracies in comparison with the empirical equation-based derived permeabilities.

Keywords: NMR, T_2 Distribution, LSBoost, Timur-Coates, Permeability.

Introduction

Permeability is of great importance in evaluating formation and deliverability prediction because it is a rock property related to the rate at which hydrocarbons can be recovered. It is common to estimate permeability using simple porosity-permeability correlation, which is usually derived from core data [1]. However, the porosity and permeability are not strongly correlated in carbonate reservoirs, which it indicates that other deciding parameters are involved [1].

The basis of NMR measurements on the rocks with a fluid is that the decay or relaxation time of the NMR signals, T_2, is directly related to the pore size.

The NMR signal detected from a fluid-bearing rock contains T_2 components from every different pore size in the measured volume [2]. Some of the petrophysical properties such as porosity, permeability, and free to bound fluid ratio can be inferred from T_2 distribution [3]. Due to the NMR's inability to log in to provide a direct measurement of permeability, several permeability models have been developed, and permeability can be calculated from the T_2 distribution data using one of two commonly accepted mathematical models:

- The free-fluid (Timur-Coates or Coates) model
- The mean-T_2 (the Schlumberger-Doll-Research (SDR)) model.

In these models, core sample measurements are necessary to refine the model by determining the correct coefficients' values and generating a customized model for local uses. These models assume that a good correlation exists between porosity, pore-throat size, and pore connectivity. This assumption is generally acceptable in sandstones, but model-derived permeabilities may not be reliable in carbonates. The Coates model and the SDR models cannot be directly used in carbonates due to the complicated pore types, structures, and a high heterogeneity degree. The current study proposes a new approach for boosting the permeability estimation in carbonate reservoirs from performing feature extraction analysis on NMR T_2 distribution and LSBoost ensemble technique [4]. The main section of the suggested process is performing feature extraction analysis on NMR T_2 distribution to

**Corresponding author:* Ali Nakhaee, Institute of Petroleum Engineering, School of Chemical Engineering, College of Engineering, University of Tehran, Tehran, Iran

E-mail addresses: anakhaee@ut.ac.ir

Received 2020-01-29, Received in revised form 2020-09-08, Accepted 2020-10-06, Available online 2021-03-16

extract parameters demonstrating a relationship with permeability [5]. The principle steps of the methodology are illustrated in Figure 1. The reliability of the technique is verified by the application of the samples from two wells at different oil fields.

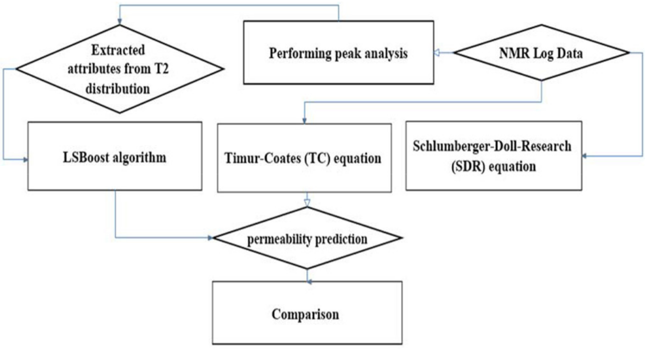

Fig. 1 Flowchart of proposed methodology.

Geological Setting

These oil fields are located in Dezful Embayment and Western Persian Gulf zones respectively, as seen in Figure 2. The Dezful Embayment is a part of the Zagros folded-thrust belt, and it contains most Iranian oilfields [6]. The Dezful Embayment borders are three faults: Mountain front fault, Balarud fault and Kazerun fault [7].

In this study, the Asmari (in field A) and Dariyan formations (in field B) were evaluated. The Asmari carbonate platform was developed during the Oligocene to Miocene [8]. This formation is deposited over the Pabdeh Formation in the southwestern part of the Zagros folded-thrust belt. However, it is mainly settled over the Jahrum formation in the Fars province. On the other hand, the Asmari Formation is present in all segments of the Zagros basin (Fig. 3), but its best development is in Dezful Embayment [9]. In the Fars province, the Asmari formation thickness is almost 180 meters, but in the Dezful Embayment, the thickness reaches 450 meters [9].

At the Early Cretaceous, a shallow carbonate platform was expanded in the Persian Gulf area [10]. The carbonate interval of the Dariyan (named as Shu'aiba in Arabian province) formation overlaid with on this platform during the Aptian [11,12,13]. In the Persian Gulf, the upper and lower contacts of the Dariyan formation are with Kazhdumi (shale) and Gadvan (marly limestone) formations respectively (Fig 3). In the Soroosh oil field, the Dariyan formation is divided into two members: the lower and upper Dariyan [14].

Materials and Methods

Materials

In this study, two wellbores from A and B oil fields were used for the permeability estimation by using NMR log data. The NMR logs were CMR type for the two wells. Dariyan and Asmari formations were studied in fields B and A, respectively. Five hundred eight core permeability data were used for the two studied wells, including 387 core permeability data from the field B and 121 core data of the field A.

Methods

NMR Log Data

Determining the T_2 distribution is of the most significant importance in NMR data analysis. This step is a mathematical inversion process called echo-fit or mapping. Due to the continuous T_2 distribution of the rock, a multi-exponential model is being utilized by the mapping process that assumes the T_2 distribution comprises m discrete relaxation times, T_{2i}, with corresponding porosity portions, ϕi. Equations (1) and (2) display the system of equations, and their matrices that present individual echoes [15].

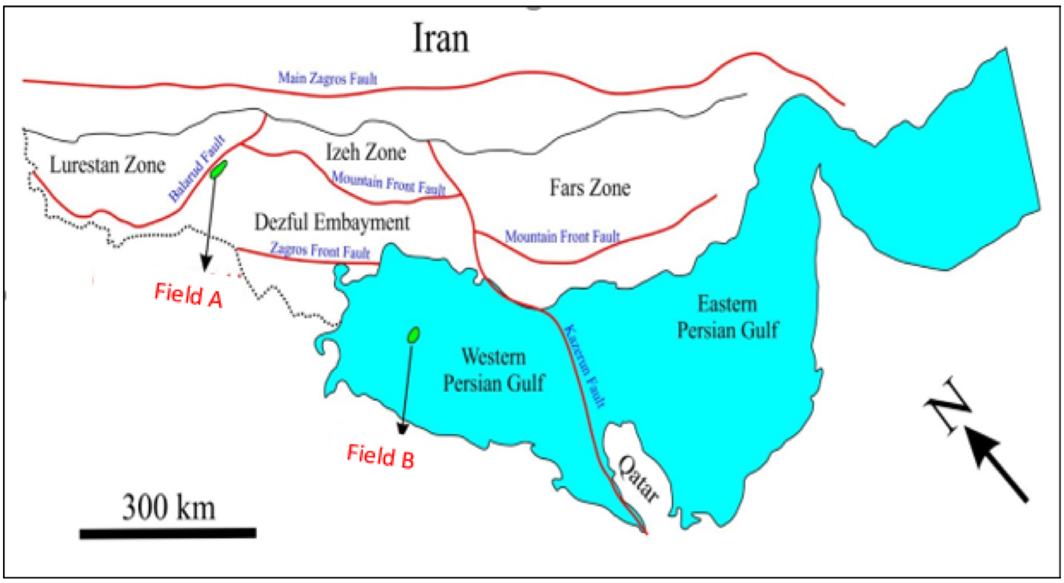

Fig 2. The studied oil fields location. Field A is located in Dezful Embayment next to the Balarud fault and field B is located in Western Persian Gulf.

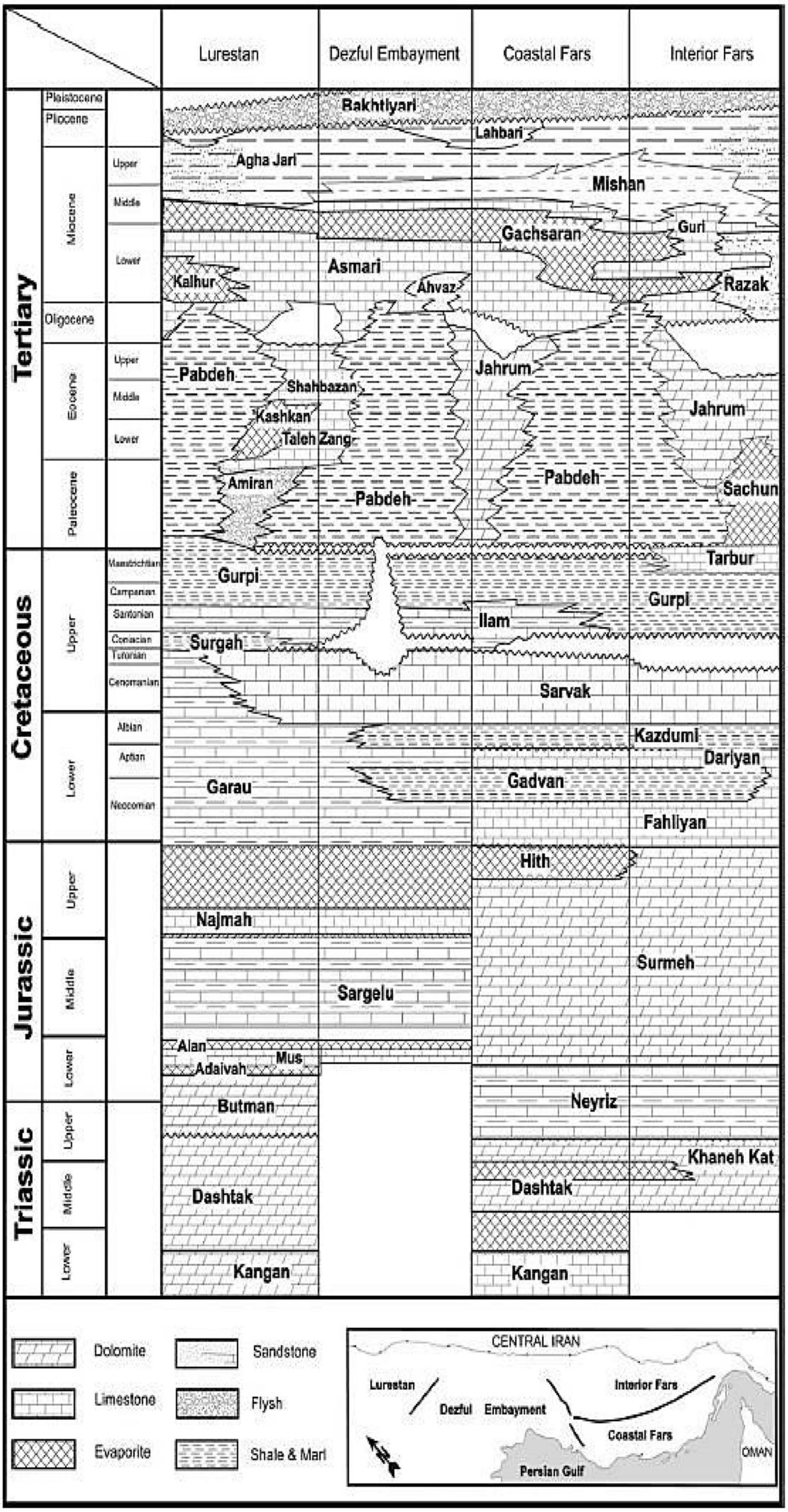

Fig. 3 The Asmari and Dariyan Formations location in the stratigraphic column of Zagros [8].

$$\begin{aligned}
Echo(1) &= \Phi_1 e^{-\left[\frac{t(1)}{T2,1}\right]} + \Phi_2 e^{-\left[\frac{t(1)}{T2,2}\right]} + \Phi_3 e^{-\left[\frac{t(1)}{T2,3}\right]} + \ldots + \Phi_m e^{-\left[\frac{t(1)}{T2,m}\right]} + noise \\
Echo(2) &= \Phi_1 e^{-\left[\frac{t(2)}{T2,1}\right]} + \Phi_2 e^{-\left[\frac{t(2)}{T2,2}\right]} + \Phi_3 e^{-\left[\frac{t(2)}{T2,3}\right]} + \ldots + \Phi_m e^{-\left[\frac{t(2)}{T2,m}\right]} + noise \\
&\vdots \\
Echo(n) &= \Phi_1 e^{-\left[\frac{t(n)}{T2,1}\right]} + \Phi_2 e^{-\left[\frac{t(n)}{T2,2}\right]} + \Phi_3 e^{-\left[\frac{t(n)}{T2,3}\right]} + \ldots + \Phi_m e^{-\left[\frac{t(n)}{T2,m}\right]} + noise
\end{aligned} \tag{1}$$

$$\begin{bmatrix} Echo(1) \\ Echo(2) \\ \vdots \\ Echo(n) \end{bmatrix} = [\Phi_1 \Phi_2 \cdots \Phi_m] \times \begin{bmatrix} e^{-\left[\frac{t(1)}{T2,1}\right]} & e^{-\left[\frac{t(1)}{T2,2}\right]} & e^{-\left[\frac{t(1)}{T2,3}\right]} & \cdots & e^{-\left[\frac{t(1)}{T2,m}\right]} \\ e^{-\left[\frac{t(2)}{T2,1}\right]} & e^{-\left[\frac{t(2)}{T2,2}\right]} & e^{-\left[\frac{t(2)}{T2,3}\right]} & \cdots & e^{-\left[\frac{t(2)}{T2,m}\right]} \\ e^{-\left[\frac{t(n)}{T2,1}\right]} & e^{-\left[\frac{t(n)}{T2,2}\right]} & e^{-\left[\frac{t(n)}{T2,3}\right]} & \cdots & e^{-\left[\frac{t(n)}{T2,m}\right]} \end{bmatrix} + noise \tag{2}$$

where t(i) is the time when the ith echo was acquired (Fig. 4).

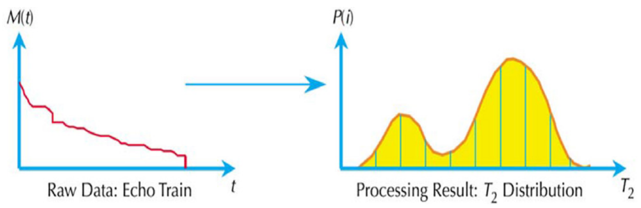

Fig. 4 The echo train (amplitude as a function of time) is mapped to a T_2 distribution [15].

Permeability Prediction Background

In recent decades, the nuclear magnetic resonance method is used to calculate permeability [5,16]. Some of the petrophysical properties such as porosity, permeability, and free to bound fluid ratio can be inferred from T_2 distribution which is directly related to the pore size [17]. Therefore, NMR logging cannot provide direct measurements of permeability. The Formation-permeability index is calculated from the spectral-porosity measurements using permeability models that are based on a combination of empirical and theoretical connections. The two established equations for deduction of permeability from NMR T_2 distribution data measurements are the free-fluid (Timur-Coates or Coates (TC)) equation [18,19]:

$$K_{TC} = a \times \left(\frac{\Phi_{NMR}}{100}\right)^4 \times \left(\frac{BVM}{BVI}\right)^2 \tag{3}$$

and the mean-T_2 (the Schlumberger-Doll-Research (SDR)) equation which was pesented by Kenyon et al in 1986 [20]:

$$K_{SDR} = b \times (\Phi_{NMR})^4 \times (T_{2\_\log mean})^2 \tag{4}$$

K_{SDR} = Schlumberger-Doll-Research permeability [md]
Φ_{NMR} = NMR measurement porosity in [*pu*]
BVM = bulk volume movable in [*pu*]
BVI = bulk volume irreducible in [*pu*]
$T_{2\_log\ mean}$ = logarithmic mean of T_2 distribution in [*ms*]
a = empirical proportionality constant in [ms^2]
b = empirical proportionality constant in [m^2/ms^2]

Performing Peak Analysis

A common requirement in scientific data processing is to detect peaks in a signal and to measure their positions, heights, widths, areas or number of peaks. In this study, the relevant peak parameters were extracted from a measured spectrum performed with MATLAB software (Signal Processing Toolbox), which offers the detection and analysis of NMR T_2 distribution signal peaks in acquired waveforms. The extracted attributes from the T_2 distribution are:

• **Peak Count**: The Peak Finder function counts the local extrema number in each row of the real-valued input signal, releasing the number of local extrema as an output.

Amplitude: The amplitude of a periodic variable is a measurement of its change over a single period (Fig. 5).

• **Width**: It is the extent of a function between the two extreme values of the variable at which the dependent variable is equal to half of its maximum value (Fig-5).

• **TCMR**: total CMR porosity, which comes from the area below the NMR T2 peaks.

• $\mathbf{T_{2lm}}$: T2 Logarithmic Mean.

• **Prominence**: the height point of a peak crest above the lowest contour line encircling it but containing no higher crest.

• **Standard Deviation**: the standard deviation is used to show the variation of the values of a data set.

• **Skewness**: in a set of statistical data, the asymmetry from the normal distribution is defined as skewness.

• **Kurtosis**: a statistical measure was used to describe data distribution around the mean (Fig.5).

Extracted relevant peak parameters are stored in separate matrixes to perform cross plot analysis versus core derived permeability values to find reliable parameters to estimate the rock permeability.

LSBoost Algorithm

As a general method, boosting can improve any learning algorithm [21,22]. Moreover, the Boosting method is one of the popular ensembles learning methods used in machine learning [23]. There are plenty of boosting algorithms, including AdaBoost, LogitBoost, GentleBoost RobustBoost.

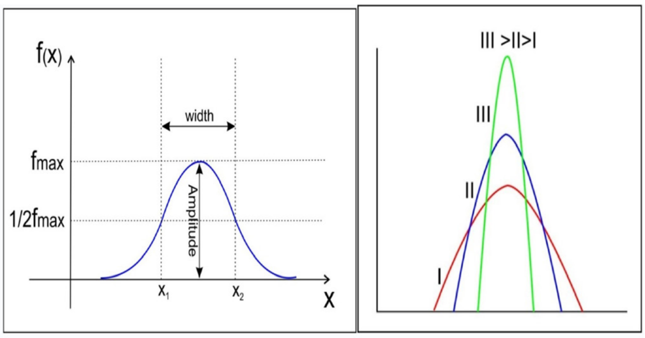

Fig. 5 The width and Amplitude of the NMR T_2 hump (left) and its Kurtosis (right).

Only LSBoost ensemble function is a suitable boosting technique for forecasting problems and regression [24], derived from the Friedman gradient-based boosting machine [25].

A 'fit ensemble' function was used by the boosting algorithm in which the weak learner has to be selected appropriately. The advantage of the boosting method lies in combining a series of weak classifiers to generate a very important "committee". It can improve accuracy with iteration. The LSBoost locates a new learner at every step to the difference between the observed and the piled prediction responses of all learners, which are grown beforehand.

The weight values through repeated training will be adjusted by LSBoost to reduce error rates. A series of regression trees, which are called weak learners (B), is used by the LSBoost to minimize the mean squared error (MSE) between variable target Y and the aggregated prediction of the weak learners (Ypred) based on the Cherkassky and Ma method, presented in 2009 [26].

The LSBoost onsets with a primitive aggregated-prediction guess of the target variable (Ỹ) median as a function of the predictor variables (X). Afterwards, it mixes multiple regression models B1, . . ., Bm in a weighted manner to boost overall predictive results [25]:

$$Y_{pred}(X) = \tilde{Y}(X) + \nu \sum_{m=1}^{M} \rho_m B_m(X) \quad (5)$$

where M is the total number of weak learners, ν with 0< ν <1 being the learning rate, and ρ_m is the weight for model m. The algorithm is briefly described in algorithm 1, where x and y represent the explanatory variable and response variable respectively. More details could be found in previous studies [27,28].

The following algorithm (Algorithm 1) is used to solve the problem, i.e. permeability estimation in carbonate reservoirs.

Algorithm 1. **The LSBoost algorithm**.

Input: A training set $\{(x_i, y_i\}^n_{i=1}$, a loss function L (y-F) = $(y-F)^2/_2$, number of iterations M

Initialize, F (x) = ȳ

For m = 1 to M do:

$\bar{y}_i = y_i - Fm\text{-}1\,(x_i),\ i=1,\ldots N_i$

$(\rho m,\ am) = \arg\min_{a,\rho} \sum^{N}_{i=1} [\tilde{Y}_i - \rho h(x_i;\ a)]^2$

$F_m(x) = F_{m-1}(x) + \rho_m h(x, a_m)$

End for

Output: The final regression function $Fm(x)$.

Results and Discussion

In this study, a prediction model was proposed to estimate the reservoir permeability. To estimate an appropriate permeability, the input layer was required to include all relevant information on the target data.

A cross plot analysis was used in this study while a trial and error input selection method was applied to identify appropriate input variables (Fig. 6).

The analysis showed a correlation coefficients of up to 0.47 between core derived permeability and NMR extracted parameters. Therefore, T_{2lm}, TCMR, prominence, peak amplitude and width variables were chosen as the input parameters for constructing the permeability estimation model (Fig. 6). In contrast, the kurtosis, standard deviation, skewness and peak counts were discarded due to their very weak association with permeability values and the trial and error input selection. At this level, the regression ensemble model (LSBoost) was constructed by MATLAB, and selected input parameters were subjected to model permeability values.

Based on the proposed technique, two wellbores located in the two different Iranian fields were processed, and the corresponding carbonate permeability was estimated. In regard to the permeability prediction, it can be observed by us that a relationship exists between T_{2lm}, TCMR, prominence, peak amplitude and width, which they were extracted from field NMR log data and measured core permeability. Such a relationship enables us to predict the permeability values by using artificial intelligence systems, leading to little errors in permeability estimation.

In Fig-7, the tracks 1 to 7 are indicating Depth, Gama Ray, Caliper-Bit Size, Neutron-Density, UBI image log, OBMI image log and T_2 distribution.

The Neutron and Density logs are overlain in the total interval, demonstrating that the main lithology is limestone. The T_2 distribution is almost bimodal, and some breakouts can be seen in the UBI image log.

Fig. 8 shows a field example of NMR data-derived attributes and permeability estimation in the well in field B. In this figure, the displayed T_{2lm} curve in the first track is the logarithmic mean of the NMR T_2 distribution, which was acquired from the CMR tool. The second track is the total CMR porosity.

Furthermore, tracks 3 to 5 show peak amplitude, width and prominence, extracted by performing peak analysis on NMR T_2 distribution curves. In the sixth track of Fig. 8, the curve of predicted permeability is shown with routine core derived permeability plotted on top of that, which is the best-compiled presentation for showing log correlations.

The correlation coefficient of core derived permeability versus LSBoost predicted permeability is displayed in Fig. 9, which is computed as 0.8833 for the well in the field B. To intuitively illustrate the improvement of permeability prediction using intelligent methods, a comparison made between acquired permeabilities from three different methods, including one inelegant-based method known as LSBoost and two empirical methods involving the Timur-Coates (or Coates) and the SDR models (Fig. 10).

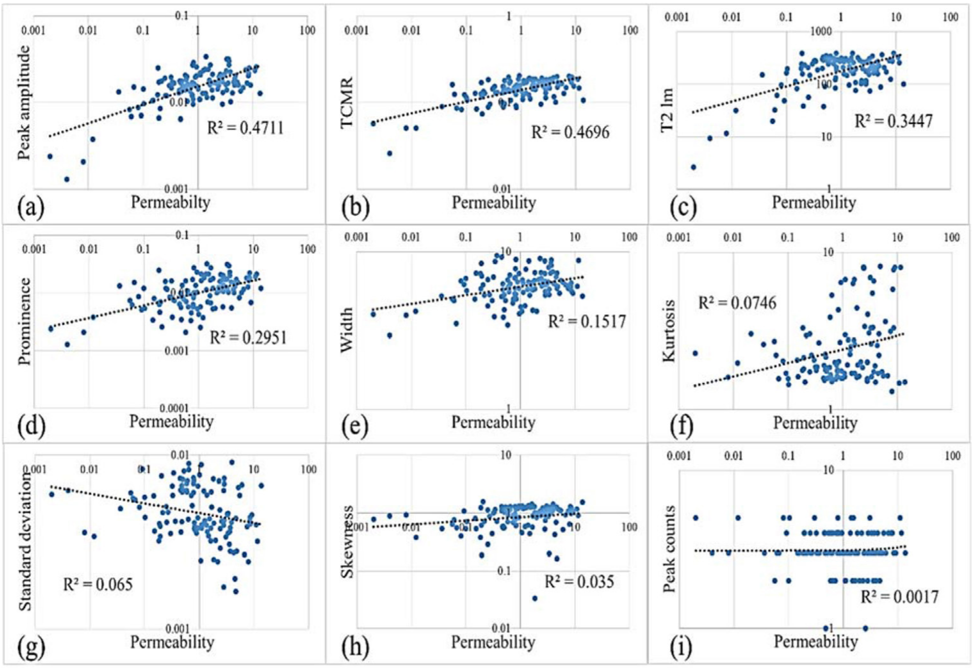

Fig. 6 Cross-plot showing the relationship between core derived permeability and peak amplitude (a), TCMR (b), T_{2lm} (c), prominences (d), width (e), kurtosis (f), standard deviation (g), skewness (h) and peak counts (i) in training.

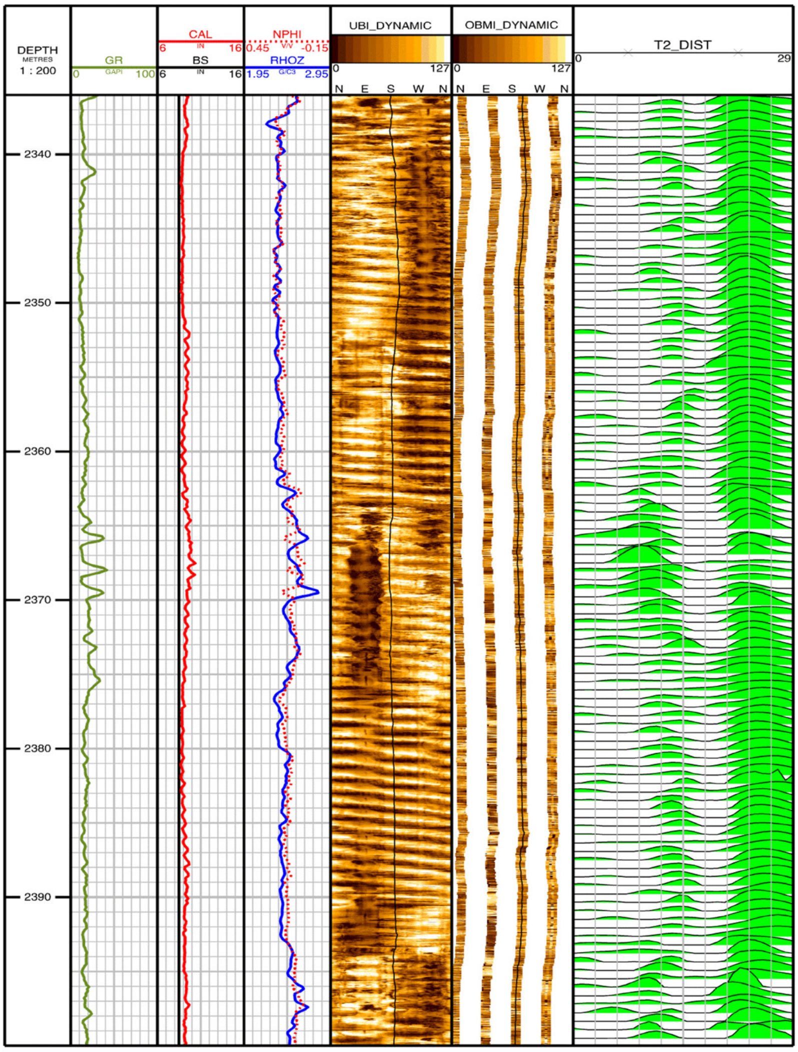

Fig. 7 The NMR T_2 distribution, Image logs and fullset data of the studied well in the field B

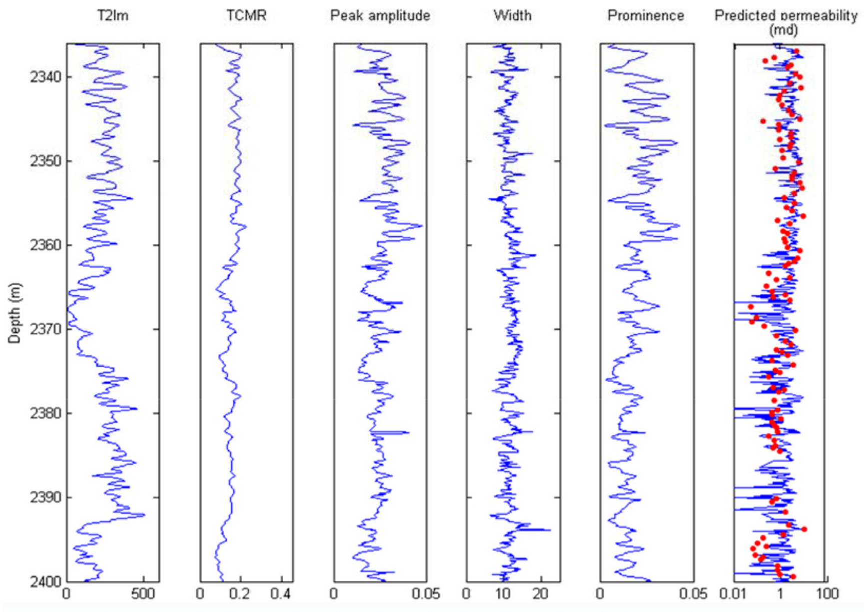

Fig. 8 The T_2 distribution attributes which used for the permeability estimation in studied well in the field B.

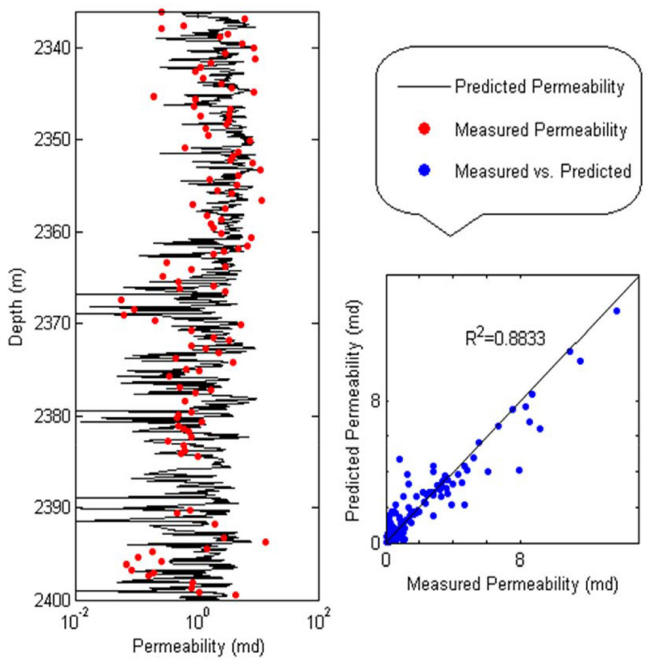

Fig. 9 The correlation between the estimated and core permeability in the field B.

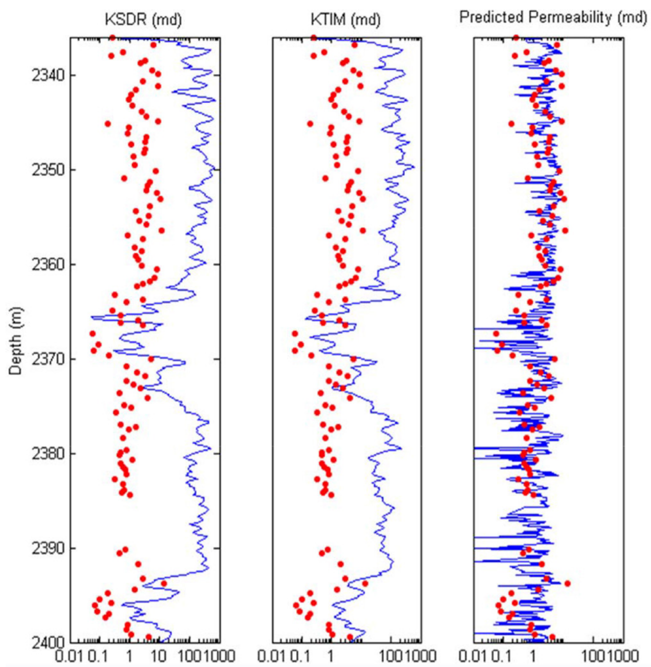

Fig. 10 Comparison of the estimated permeability with the SDR and Coates methods of the well 31in the field B.

Demonstrated results in Fig-10 indicate that there are large discrepancies between the core derived and SDR and Coates derived permeabilities. In both types of models, permeabilities are overestimated. Hence, it can be inferred that in carbonates, empirical model-derived permeabilities could not be reliable. However, the third track of the Fig. 10 shows that predicted permeabilities using the LSBoost method are appropriately matching the core derived ones. From these comparisons, it can be observed that LSBoost model outperform the SDR and Coates permeability derived models , as seen in Fig. 11.

In Fig. 12, the tracks 1 to 5 are indicating Depth, Gama Ray, Caliper-Bit Size, Neutron-Density and NMR T_2 distribution. These well data are related to the field A. The main lithology in this interval is dolomite, and the wellbore wall condition is very good. The NMR-derived attributes and estimated permeability by using the boosting are shown in Fig. 13. The correlation coefficient between the estimated and core permeability is 0.8588 in this well (Fig. 14).

As can be seen in Fig. 15, the SDR and Coates derived permeabilities are closer to core permeability (compared to the well in the field B), but the estimated permeability by using the boosting method is more consistent with core permeability. The cross plot of different methods in this well is shown in Fig. 16. The experimental results available in the literature show that this regression model outperforms other existing models by representing a good matching between measured and predicted values, resulting in bigger values for R-squared [4,29, 30, 31].

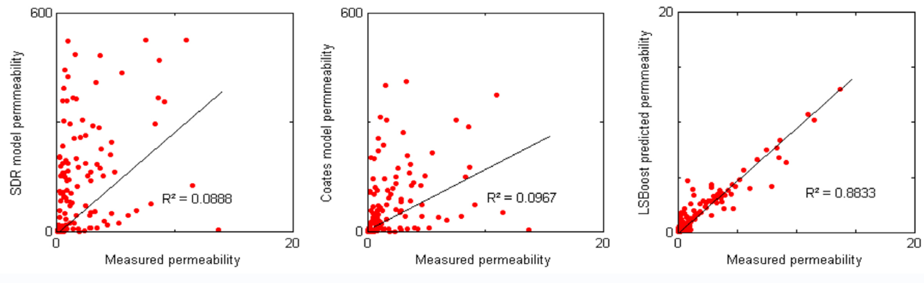

Fig. 11 Comparison the correlation of the estimated permeability with the SDR and Coates methods of the well in the field B.

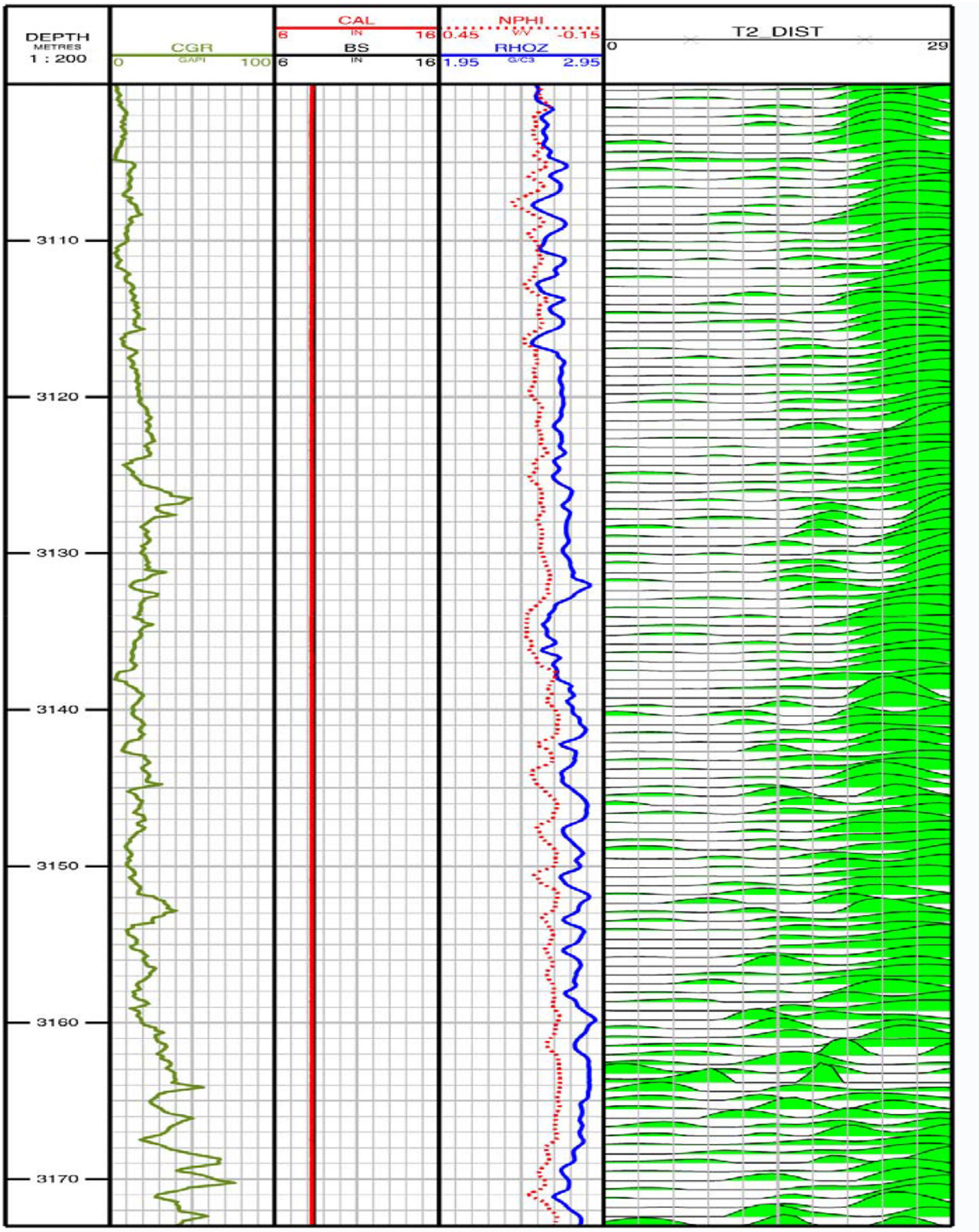

Fig. 12 The NMR T_2 distribution and fullset data of the studied well in the field A.

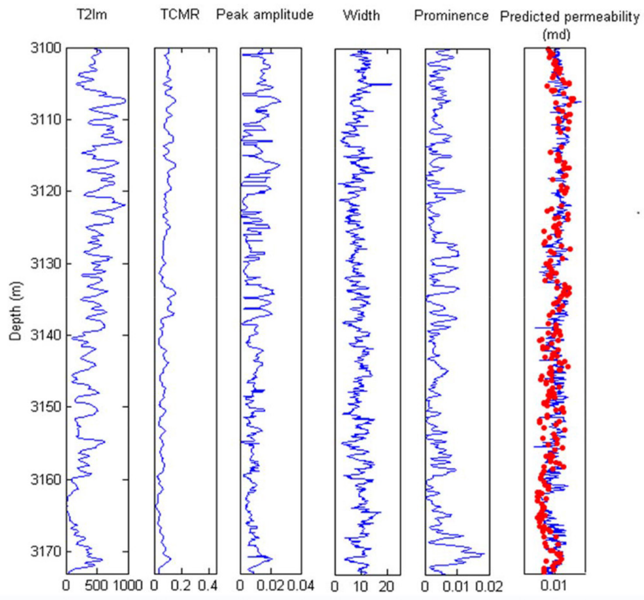

Fig. 13 The T_2 distribution-derived parameters which used for the permeability estimation in studied well in the field A.

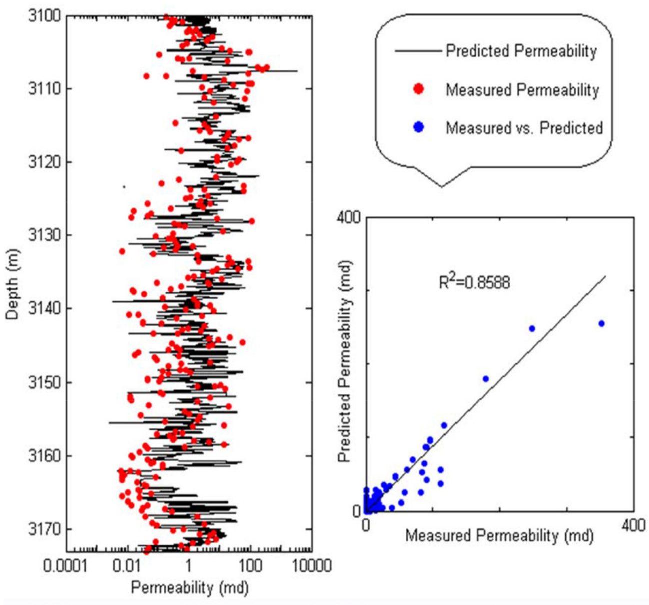

Fig. 14 The correlation between the estimated and core permeability in the studied well in the field A.

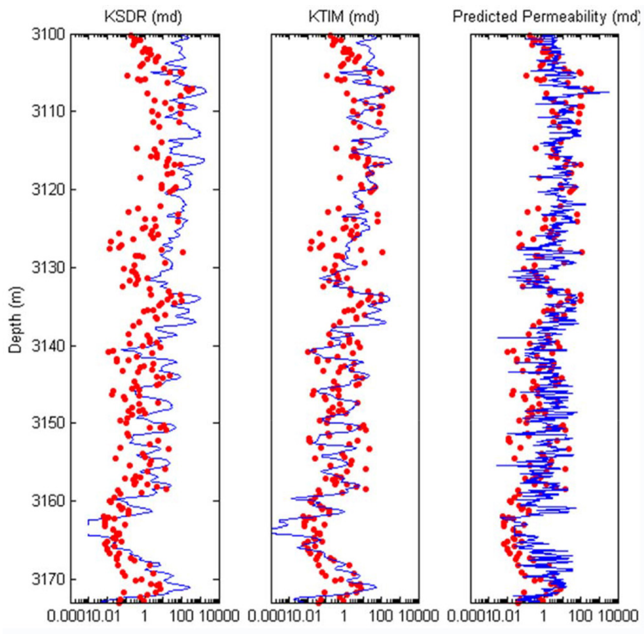

Fig. 15 Comparison of the estimated permeability with the SDR and Coates methods in the in the field A.

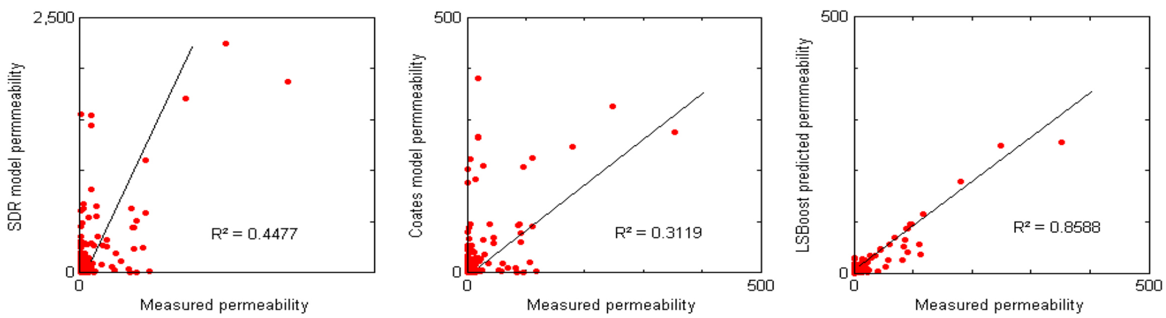

Fig. 16 Correlation of the estimated permeability with the SDR and Coates methods in the field A.

Conclusions

Carbonate reservoirs are invariably heterogeneous due to the complex depositional and diagenetic environments. In most of the carbonate reservoirs, fluid flow characteristics are generally difficult to predict, and equation-derived permeabilities may not be reliable. In this study, a new technique is proposed for predicting the permeability from NMR data. According to the best of our knowledge, this is the first time, the peak analysis was applied to NMR T_2 distribution to do the permeability forecasting while being integrated with boosting regression. Moreover, it was shown that in comparison with KSDR and KTC methods, the proposed method could significantly improve prediction accuracy. The new method was derived by considering the link between the extracted features from T_2 distribution, including T_{2lm}, TCMR, prominence, peak amplitude and width and core derived permeability in a porous medium. It was formulated using LSBoost ensemble regression algorithm as a new application of machine learning method in the analysis of intricate geological data. Extracted features are obtained by performing peak analysis on the T_2 distribution NMR log data. The resulting permeability prediction was a satisfactory match with the core derived permeability with a correlation coefficient of 0.85 and 0.88 in fields A and B. The results are better than permeability predictions resulting from the free-fluid (Timur-Coates or Coates) equation (R_2 of 0.09 and 0.31 in the fields B and A respectively) or the SDR equation (R_2 of 0.08 and 0.44 in fields B and A respectively). Consequently, it could be said from quantitative comparisons of the estimated permeability and core derived permeabilities that the use of boosting ensemble methods generates more accurate predictions than equation-based methods.

Nomenclatures

MSE: Mean squared error

NMR: Nuclear magnetic resonance

References

1. Lucia F J (2007) Carbonate reservoir characterization: an integrated approach, 1st ed., Springer Science and Business Media, 1-336.
2. Dunn KJ, LaTorraca GA, Warner JL, Bergman DJ (1994) On the calculation and interpretation of NMR relaxation time distributions, In SPE Annual Technical Conference and Exhibition, Society of Petroleum Engineers.
3. Jianwei D (2015) Permeability characterization and prediction in a tight oil reservoir, Edson Field, Alberta, PhD thesis, University of Calgary, 113.
4. Cai J, Kai X, Yanhui Z, Fang H, Liuhuan L (2020) Prediction and analysis of net ecosystem carbon exchange based on gradient boosting regression and random forest, Applied energy, 262: 114566.
5. Aghda, S. F., Taslimi, M., & Fahimifar, A. (2018). Adjusting porosity and permeability estimation by nuclear magnetic resonance: a case study from a carbonate reservoir of south of Iran. Journal of Petroleum Exploration and Production Technology, 8, 4: 1113-1127.
6. Bordenave ML, Hegre JA (2010) Current distribution of oil and gas fields in the Zagros Fold Belt of Iran and contiguous offshore as the result of the petroleum systems, Geological Society, London, Special Publications, 330, 1: 291-353.
7. Sepehr M, Cosgrove JW (2004) Structural framework of the Zagros fold–thrust belt, Iran, Marine and petroleum geology, 21, 7: 829-843
8. Homke S, Jaume V, Miguel G, Hadi E, Ridvan K (2004) Magnetostratigraphy of Miocene–Pliocene Zagros foreland deposits in the front of the Push-e Kush arc, Lurestan Province, Iran, Earth and Planetary Science Letters, 225, 3: 397-410.
9. Motiei H (1993) Stratigraphy of Zagros, Treatise on the Geology of Iran, 60: 151.
10. Alsharhan AS, Nairn AEM (1993) Carbonate platform models of Arabian Cretaceous reservoirs, 173-184.
11. Schroeder R, Frans SP van B, Antonietta C, Darioush B, Benoit V, Adrian I, Bruno G (2010) Revised orbitolinid biostratigraphic zonation for the Barremian–Aptian of the eastern Arabian Plate and implications for regional stratigraphic correlations, GeoArabia Special Publication 4, 1: 49-96.
12. Droste H (2010) High-resolution seismic stratigraphy of the Shu'aiba and Natih formations in the Sultanate of Oman: implications for Cretaceous epeiric carbonate platform systems, Geological Society, London, Special Publications, 329, 1: 145-162.
13. MMaurer F, Van Buchem FS, Eberli GP, Pierson BJ, Raven MJ, Larsen PH, Al-Husseini MI, Vincent B (2013) Late Aptian long-lived glacio-eustatic lowstand recorded on the Arabian Plate. Terra Nova, 25, 2: 87-94.
14. Mehrabi H, Rhimpour-Bonab H, Hajikazemi E, Esrafili-Dizaji B (2015) Geological reservoir characterization of the Lower Cretaceous Dariyan Formation (Shu'aiba equivalent) in the Persian Gulf, southern Iran, Marine and Petroleum Geology, 68: 132-157.
15. Coates GR, Xiao LI ZHI, Prammer MG (1999) NMR logging. Principles and Applications, 1st ed., Halliburton Energy Services Publication, 1-227.
16. Lis-Śledziona A (2019) Petrophysical rock typing and permeability prediction in tight sandstone reservoir, Acta Geophysica, 67, 6: 1895-1911.
17. Lu Z, Sha A, Wang W (2020) Permeability evaluation of clay-quartz mixtures based on low-field NMR and fractal analysis, Applied Sciences, 10, 5: 1585.
18. Timur A (1968) An investigation of permeability, porosity, and residual water saturation relationships. In: SPWLA 9th annual logging symposium, New Orleans, Louisiana, Society of Petrophysicists and Well-Log Analysts.
19. Coates G R, Denoo S (1988) The producibility answer product, Schlumberger Technical Review, 29, 2: 55.
20. Kenyon WE, Day PI, Straley C, Willemsen J (1986) Compact and consistent representation of rock nmr data for permeability estimation, paper SPE 15643.
21. Freund Y, Schapire RE (1996) Experiments with a new boosting algorithm, In Proceedings of the Thirteenth International Conference on International Conference on Machine Learning (ICML), Bari, Italy, 3–6: 148–156.
22. Schapire RE (2003) The boosting approach to machine learning: an overview nonlinear estimation and

classification, Springer: New York, NY, USA, 149–171.
23. Bishop CM (2007) Pattern recognition and machine learning, Springer: New York, NY, USA, 1–738.
24. Su M, Zhang Z, Zhu Y, Zha D (2019) Data-driven natural gas spot price forecasting with least squares regression boosting algorithm, Energies, 12, 6: 1094; https://doi.org/10.3390/en12061094.
25. Jung C, Schindler D (2015) Statistical modeling of near-surface wind speed: a case study from Baden-Wuerttemberg (Southwest Germany), Austin Journal of Earth Science2, 1: 1006.
26. Cherkassky V, Ma Y (2009) Another look at statistical learning theory and regularization. Neural Networks, 22, 7: 958-969.
27. Bianco V Manca O, Nardini S (2009) Electricity consumption forecasting in Italy using linear regression models, Energy, 34: 1413–1421
28. Breiman L (2001) Random forests, Machine Learning, 45, 5–32.
29. Dargahi Zarandia A, Hemmati Sarapardehb A, Shateric M, Menad NA, Ahmadi M (2020) A modeling minimum miscibility pressure of pure/impure CO_2-crude oil systems using adaptive boosting support vector regression: Application to gas injection processes, Journal of Petroleum Science and Engineering, 184: 106499, https://doi.org/10.1016/j.petrol.2019.106499
30. Wang FK, Mamo T (2020) Gradient boosted regression model for the degradation analysis of prismatic cells, Computers and Industrial Engineering, doi:https://doi.org/10.1016/j.cie.2020.106494
31. Li X, Zhang L, Wang Z, Dong P (2019) Remaining useful life prediction for lithium-ion batteries based on a hybrid model combining the long short-term memory and Elman neural networks, Journal of Energy Storage, 21, 510-518.